MESSENGER VIEWS OF CRATER RAYS ON MERCURY. Noam R. Izenberg[1], David T. Blewett[1], Ralph L. McNutt[1], Nancy L. Chabot[1], Clark R. Chapman[2], Brett W. Denevi[3], Mark S. Robinson[3], Louise M. Prockter[1], and Scott L. Murchie[1]. [1]Johns Hopkins University Applied Physics Laboratory, 11100 Johns Hopkins Road, Laurel, MD, 20723, USA (noam.izenberg@jhuapl.edu). [2]Southwest Research Institute, 1050 Walnut Street, Boulder, CO 80302, USA. [3]School of Earth and Space Exploration, Arizona State University, Tempe, AZ 85287, USA.

Introduction: First-order albedo variations on Mercury, which lacks the highland/mare reflectance contrasts of the Moon, are largely related to differences in regolith maturity. High-reflectance crater materials and extensive ray systems are particularly notable on the portion of the planet imaged during MESSENGER's second Mercury flyby. MESSENGER images provide the opportunity to make comparisons with lunar rays and with Earth-based radar images of Mercury.

The Nature of Crater Rays: Three types of lunar crater rays have been recognized [1]: (a) "immaturity rays," which exhibit high reflectance because of the presence of fresh material that has been little affected by the darkening associated with exposure to the space environment [e.g., 2, 3]; (b) "compositional rays," which are visible because of a composition (and hence albedo) contrast with the surroundings unrelated to the state of maturity; and (c) "combination rays," which are characterized by an albedo contrast arising from both a difference in inherent composition and a difference in the state of maturity between the ray and substrate material.

Major Ray Systems: During the second flyby of Mercury, the Mercury Dual Imaging System (MDIS) collected images of the planet with the multispectral Wide Angle Camera (WAC) and the monochrome Narrow Angle Camera (NAC). Three especially prominent ray systems were documented.

Kuiper. The crater Kuiper (~62-km diameter, 11°S, 329°E) was one of the highest-reflectance features imaged by Mariner 10 [4]. Analysis of Mariner 10 two-color images suggested that the Kuiper rays owe their high reflectance primarily to the presence of immature material, though low opaque abundance (a compositional factor) could play some role [5, 6], i.e., Kuiper's rays are of the "combination" variety, though immaturity is the dominant cause of the ray's high reflectance. The MESSENGER NAC image in Fig. 1 illustrates the bright halo surrounding Kuiper to a distance of about one crater diameter and the ray segments extending outward from the halo. Some of the high-reflectance material just southeast of Kuiper's rim (on the floor of the older crater Murasaki) could be related to the presence of pyroclastic deposits. Fig. 1 (arrows) shows what may be shallow irregular depressions on the floor of Murasaki. A WAC color-composite image (Fig. 1 inset) makes it clear that red, low-opaque material is present on Murasaki's floor adjacent to the rim of Kuiper, in the area around the possible irregular depressions. Elsewhere on Mercury, WAC multispectral images have revealed a number of diffuse red deposits associated with irregular depressions; these have been interpreted as pyroclastic deposits [7-11]. Thus Kuiper may resemble the crater Aristarchus on the Moon, another bright, young, rayed crater that formed on a pre-existing pyroclastic deposit.

Radar "A". To the southeast of Kuiper, in a portion of the planet not viewed by Mariner 10, lies a dramatic rayed crater known from Earth-based radar observations [12]. Approximately 85 km in diameter and centered at ~33.8°S, 12.2°E, this crater is referred to as radar feature "A." Crater features revealed in NAC imagery (Fig. 2) include high-reflectance material on the rim (likely excavated from the greatest depth) and a bright halo extending one to two crater diameters from the rim. These features are seen in 12.6-cm same-sense radar images [12]. A "swallow-tail" exclusion zone in the ray pattern extends from "A" toward Kuiper, possibly indicating that the "A" impactor approached from the northwest at a relatively low angle [e.g., 13]. Rays of "A" interfinger with those of Kuiper near 19°S, 336°E, and may extend all the way to Kuiper itself – a distance of over 1900 km. Maps of multispectral compositional and optical maturity parameters [7, 10] suggest that there is a compositional contrast between the rays of "A" and their surroundings, particularly with the low-reflectance material (LRM – 7, 10, 14, 15) to the east and south of the crater. The proximal, continuous halo around the crater has a different appearance in multispectral parameter images than the more distal rays, also indicative of compositional differences. Thus the rays of "A" are predominantly immaturity rays, with some of their visibility attributable to compositional contrast.

Radar "B". A second feature prominent in Earth-based radar images of Mercury is located at ~57.8°N, 16.8°E. The ambiguous form of this feature "B" in initial radar images led to early speculation that it could be a shield volcano [16], but improved radar capabilities demonstrated that "B" is in fact a fresh impact crater [12]. Feature "B" occurs near the northeast limb in MESSENGER second flyby departure images (Fig. 3). Crater "B" is ~100 km in diameter and

its rim is composed of LRM. A high-reflectance halo of one to two crater diameters surrounds "B," similar to the halos of Kuiper and radar "A." Most surprising is the crater's enormous bright ray system, which is even more spectacular than that of "A." Rays from "B" cross Kuiper and the proximal rays of "A," thus extending to great-circle distances of at least 4500 km. For comparison, rays of the lunar crater Tycho reach the Apollo 17 landing site, a distance of ~2200 km. Photometric effects limit color interpretations on the limb near "B" itself, but the rays of this crater certainly owe the majority of their visibility to immaturity. Where a ray segment from "B" crosses the rays of "A," the "B" ray displays differing spectral character (Fig. 2 inset). At this great distance from the primary "B" impact, secondary crater-forming projectiles would be expected to excavate many times their own mass, with the resulting ray deposit dominated by redistributed local material [17]. The rays of "A" at this location would contain a greater proportion of primary ejecta.

Conclusions: MESSENGER has collected images of prominent rayed craters on Mercury, greatly augmenting data from Mariner 10 and Earth-based radar. Integrated analysis of these data will offer new insight into the cratering process, ejecta deposition, crustal stratigraphy, and regolith maturation.

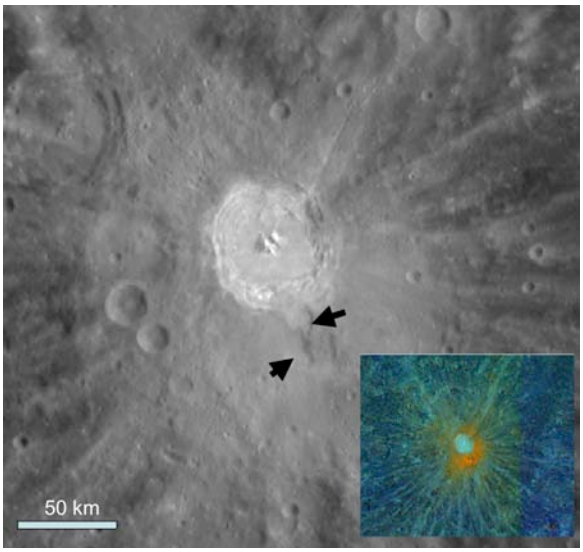

Figure 1. Kuiper and Murasaki in a NAC image centered near 12.2°S, 329.2°E. Arrows show irregular depressions on the floor of Murasaki. Inset: WAC composite parameter image. Red = inverse opaque index [5, 6, 10] (brighter = lower opaques). Green = near-infrared optical maturity parameter [10], brighter = less mature). Blue = color ratio (430 nm/750 nm, brighter = less red).

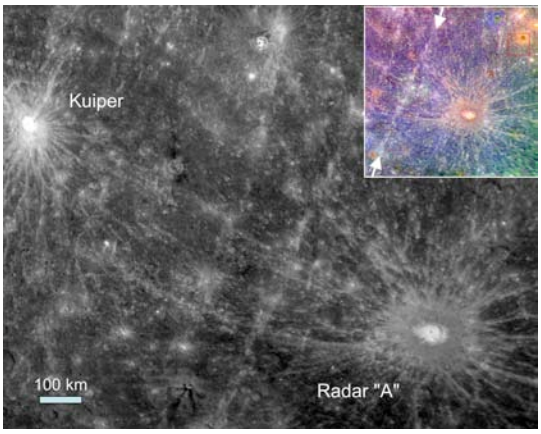

Figure 2. NAC mosaic in simple cylindrical projection, centered at ~22°S, 354°E. Inset: WAC composite parameter image of "A" (same color assignments as Fig. 1, different stretch). Arrows show segment of ray from Radar "B," for comparison with Fig. 3.

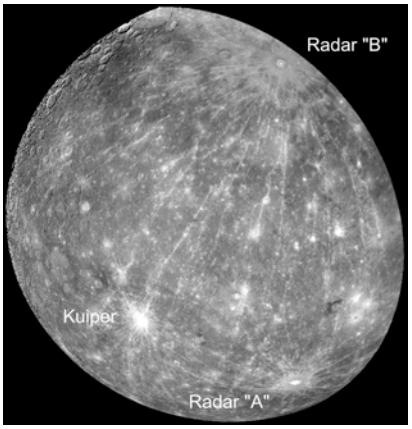

Figure 3. NAC mosaic in orthographic projection centered at 24°N, 352°E (roughly midway between Kuiper and radar "B").

References: [1] B. R. Hawke et al. (2004), *Icarus 170*, 1. [2] B. Hapke (2001), *JGR 106*, 10,039. [3]S. K. Noble and C. M. Pieters (2003), *Solar System Res. 37*, 31. [4] B. Hapke et al. (1975), *JGR 80*, 2431. [5] M. S. Robinson and P. G. Lucey (1997), *Science 275*, 197. [6] D. T. Blewett et al. (2007), *JGR 112*, E02005. [7] M. S. Robinson et al. (2008), *Science 321*, 66. [8] J. W. Head et al. (2008), *Science 321*, 69. [9] S. L. Murchie et al. (2008), *Science 321*, 73. [10] D. T. Blewett et al. (2008), *EPSL*, submitted. [11] L. Kerber et al. (2008), *EPSL*, submitted. [12] J. K. Harmon et al. (2007), *Icarus 187*, 374. [13] R. R. Herrick and N. K. Forsberg-Taylor (2003), *MPS 38*, 1551. [14] B. W. Denevi et al. (2008), *Eos Trans. AGU 89*, Fall Mtg. Suppl., U21A-0025. [15] M. A. Riner et al. (2009), *GRL*, in press. [16] J. K. Harmon (1997), *Adv. Space Res. 19*, 1487. [17] V. R. Oberbeck (1975), *Rev. Geophys. 13*, 337.